Challenges and Opportunities for the Clinical Translation of Spatial Transcriptomics Technologies

Kelly D. Smith[a]   David K. Prince[b]   James W. MacDonald[c]   Theo K. Bammler[c]
Shreeram Akilesh[a, b]

[a]Department of Laboratory Medicine and Pathology, University of Washington, Seattle, WA, USA; [b]Kidney Research Institute, Seattle, WA, USA; [c]Department of Environmental and Occupational Health Sciences, University of Washington, Seattle, WA, USA

Abstract

Background: The first spatially resolved transcriptomics platforms, GeoMx (Nanostring) and Visium (10x Genomics) were launched in 2019 and were recognized as the method of the year by *Nature Methods* in 2020. The subsequent refinement and expansion of these and other technologies to increase -plex, work with formalin-fixed paraffin-embedded tissue, and analyze protein in addition to gene expression have only added to their significance and impact on the biomedical sciences. In this perspective, we focus on two platforms for spatial transcriptomics, GeoMx and Visium, and how these platforms have been used to provide novel insight into kidney disease. The choice of platform will depend largely on experimental questions and design. The application of these technologies to clinically sourced biopsies presents the opportunity to identify specific tissue biomarkers that help define disease etiology and more precisely target therapeutic interventions in the future. *Summary:* In this review, we provide a description of the existing and emerging technologies that can be used to capture spatially resolved gene and protein expression data from tissue. These technologies have provided new insight into the spatial heterogeneity of diseases, how reactions to disease are distributed within a tissue, which cells are affected, and molecular pathways that predict disease and response to therapy. *Key Message:* The upcoming years will see intense use of spatial transcriptomics technologies to better define the pathophysiology of kidney diseases and develop novel diagnostic tests to guide personalized treatments for patients.

© 2024 The Author(s).
Published by S. Karger AG, Basel

Introduction

Though there has been intense effort to identify noninvasive, blood- and urine-based biomarkers, the renal biopsy remains the gold standard to diagnose kidney diseases, guide treatment decisions, and inform prognosis. All major structures of the nephron such as glomeruli, tubules, interstitium, and vasculature are systematically evaluated by diagnostic laboratories. The keystone of the pathologic evaluation of biopsies rests on formalin-fixed paraffin-embedded (FFPE) tissue, which is

Correspondence to:
Shreeram Akilesh, shreeram@uw.edu

subjected to multiple histologic stains, including Jones methenamine silver, periodic acid-Schiff, hematoxylin and eosin, and trichrome. These stains label different components of the tissue to help delineate the kidney architecture. The findings from the light microscopic evaluation are then integrated with those gained from evaluation of separate portions of the biopsy tissue by immunofluorescence and electron microscopy to arrive at the final clinicopathologic assessment. Numerous biopsy-based classification and grading schemes leverage this general approach to standardize reporting of findings in glomerular diseases (e.g., lupus nephritis, membranous nephropathy, diabetic kidney disease, IgA nephropathy, pauci-immune glomerulonephritis) and transplant rejection (Banff classification). Recently, new technologies permit the addition of a "molecular layer" over this traditional histologic evaluation, which may include gene expression or protein level information. This high-dimensional molecular layer, which includes the simultaneous measurement of 100's–1,000's of analytes, can synergize with traditional histologic evaluation to reveal new biologic insights and understanding of disease processes. In this review, we will focus on one of these approaches, spatial transcriptomics, in which the expression of thousands of genes can be quantified and localized within the tissue context. We will discuss the conceptual approach to the key methods, the main commercial platforms being utilized, how insights into kidney disease have been gained, and challenges and opportunities for deploying this technology more routinely to improve patient care.

Strategies to Quantify Gene Expression in Tissue

Even beyond the targeted inquiries that can be performed with special histochemical stains (e.g., Congo red for amyloid) or immunohistochemistry or in situ hybridization (ISH) approaches, it has long been understood that there is a substantial amount of information within the tissue that remains invisible. Appreciating that human tissue represents an information-dense resource to learn about kidney health and disease, the Kidney Precision Medicine Project (KPMP) and Human Biomolecular Atlas Program (HuBMAP) are multi-year and multi-institutional endeavors to extract maximal information from kidney and other human tissues using advanced multi-omic approaches [1, 2]. Of the various methods utilized by KPMP and HuBMAP, gene expression profiling by high-throughput sequencing has been the most widely deployed. This has been facilitated

by robust sequencing-based workflows (i.e., RNA-seq) that quantify the expression levels of all ~20,000 genes in the genome. Bulk RNA-seq has had a long track record of generating insights into kidney health and disease in both human tissues and model organisms. Advances in droplet-based sequencing technology have permitted quantification of gene expression at the single-cell level (single-cell and single-nucleus RNA-seq, scRNA-seq, and snRNA-seq, respectively). These technologies have been applied to create comprehensive atlases of cell types and cell states in the kidney and other organ systems. Advanced computational approaches and orthogonal validation methods can be used to infer spatial mapping information from scRNA-seq data [3–6]. However, in their essence, both bulk and single-cell RNA-seq are dissociative approaches, meaning that they disrupt normal tissue architecture during the process of data generation. As a result, these methods lose all information about the spatial localization of gene signatures within the complex architecture of the organ. However, disease processes can show specific and heterogeneous patterns of localization within the tissue, and to address this need, several spatial transcriptomic profiling technologies have been developed, as described in the next section. These technologies enable simultaneous deep profiling of transcripts and localization of those gene signatures within a single section of tissue. An analogy showing the conceptual advantages of spatially localized gene expression profiling is shown in Figure 1. Spatial mapping of molecular signatures promises to define how specific kidney structures/regions and cells interact during healthy and diseased states and to understand the contribution of spatial heterogeneity to disease. Adding spatial context to molecular signatures in kidney tissue could help to identify novel state/transition markers, molecular pathways, disease mechanisms, biomarkers of injury, and predictors of treatment and outcome.

Methodologies to Localize Gene Expression in Tissue

Spatially localized gene expression profiling requires three essential steps: (1) detection/capture of the target gene mRNA, (2) encoding of spatial positioning on the tissue slice, and (3) readout of gene expression. In the simplest scheme, detection of the specific sequence of a target gene messenger RNA (mRNA) within a tissue section can be achieved by hybridizing a complementary DNA (cDNA) oligonucleotide (ISH). While only 1 or 2 gene targets are readily visualized by light microscopy using chromogenic readouts, many more target genes can

Smith/Prince/MacDonald/Bammler/
Akilesh

Fig. 1. Advantages of spatially localized transcriptomic analysis (using beans as an analogy). In bulk RNA-seq, the entire tissue and all its component cells are homogenized, and a single expression signature is obtained. In single-cell RNA-seq, the expression signatures of individual cells comprising a tissue can be identified. However, the location of cells within the tissue is lost during the procedure, and rare and difficult-to-isolate cells (e.g., podocytes) may be underrepresented as an artifact of tissue dissociation. Spatial transcriptomics aims to achieve single-cell resolution of expression signatures in addition to spatial registration of each cell within its native tissue context. Since only a single tissue section is needed, the method is tissue-sparing, and artifacts due to cellular dissociation or loss of rare cell types are eliminated. Image created using DALL-E2.

be detected using multiplexed fluorescent ISH (i.e., RNA-FISH). Since the fluorescent signal from a given target mRNA is usually weak, a variety of approaches have been used for signal amplification such as tiled oligonucleotides, branched DNA amplification, primer extension reaction, and rolling circle amplification [7–11]. In RNA-FISH experiments, direct visualization and imaging provide the spatial positioning information of the target gene within the tissue. However, simultaneous detection of >10–12 target genes becomes difficult using microscopic imaging alone. This "-plex" limit can be overcome using sequential detection, in which a subset of labeled targets is visualized using a small palette of detection oligonucleotides conjugated to fluorophores. After image capture, the bound oligonucleotides are stripped, and another round of detection reagents is applied to detect the next set of target genes. MERFISH is another approach that leverages sequential hybridization and imaging of fluorescent oligonucleotides to detect thousands of mRNA targets in tissue. Another approach termed FISSEQ uses probe-based detection and amplification of targets in situ coupled with a sequencing-based imaging readout. Both of these methods provide single-cell resolution but require advanced microfluidics platforms and high-end fluorescent microscopes [11–19]. A different approach involves target mRNA binding with a complementary oligonucleotide which is attached to a barcode oligonucleotide via an ultraviolet (UV) light cleavable linker. Using a precision digital micromirror to focus UV illumination to specific areas (regions of interest [ROI]) of a tissue section, barcodes attached to tissue mRNAs can be released and aspirated by a microcapillary pipette. These barcodes can be collected and converted into a next-generation sequencing compatible library for direct counting. In this way, barcodes (a surrogate for bound detection oligonucleotides) can be mapped to ROIs to provide a digital readout of gene expression within the tissue context. This approach has been implemented as a commercialized platform in the GeoMx Digital Spatial Profiler (DSP) produced by NanoString [20].

All the approaches listed above require knowledge of the target mRNA sequence and optimal design of detection oligonucleotides to ensure high specificity for their targets. An alternative approach is to capture all tissue mRNA via their polyadenylated (poly(A)) 3′ tails and then convert them into cDNA for eventual sequencing-based quantification. Several commercialized strategies are able accomplish this. In the first approach, barcoded poly(dT) deoxyribonucleotides are printed as spots onto a special slide (initially called spatial transcriptomics, now 10x Visium) [21, 22]. A second approach, termed Slide-seq, and a higher resolution follow on version called Slide-seq V2, use a dense monolayer array of barcoded beads to capture mRNAs [21–25]. A third approach called Stereo-seq uses an array of DNA nanoballs affixed to a slide to capture cellular mRNAs [26–29]. Compared to the 10x Visium implementation of

spatial transcriptomics and Slide-seq, the Stereo-seq approach is able to capture much larger tissue areas and can be combined with serial sectioning to generate spatial transcriptomic data in reconstructed 3D tissues. In all 3 approaches, after a tissue slice is applied on top of the array, mRNA diffuses from the tissue and is captured by the poly(dT) spots/beads/nanoballs. During reverse transcription of the captured mRNA, the barcode defining the spatial position of capture spot is encoded into the resulting cDNA. The resulting spatially barcoded cDNAs are pooled for next-generation sequencing and eventually mapped to their tissue location using bioinformatic approaches. The barcoded spot approach has been commercialized by 10x Genomics as the Visium platform, in which the capture spots are 55 μm in size. The bead-based approach Slide-seq has been commercialized by Curio Bioscience and has a reported resolution of 10 μm (Slide-seqV2 with a resolution of 2 μm has not yet been commercially released). The DNA nanoball-based capture strategy has been commercially deployed by BGI Genomics with individual nanoballs sized on the order of ~200 nm.

Comparison of Two Commercially Available Spatial Transcriptomics Platforms

It is evident from the previous discussion that there are now many methods to spatially localize gene expression within tissues. All of these are technically complex, though many of these are now being released as commercial platforms which has facilitated their utilization. The two earliest commercialized platforms were the 10x Genomics Visium and the Nanostring GeoMx DSP. Both 10x Visium and Nanostring GeoMx DSP systems are now available in many institutions, and the novel data that they have generated have resulted in hundreds of publications. However, these two systems use very different approaches to provide spatially localized gene expression in tissue sections. Given their widespread availability and proven ability to generate spatial transcriptomic data, it is important for the investigator to understand their relative strengths, weaknesses, and costs in order to choose the best platform suited to answer the biological question that they wish to answer (summarized in Table 1).

The original 10x Genomics Visium platform uses unbiased capture of mRNA poly(A) tails onto a barcoded spot array and therefore can be adapted to tissues from a variety of model organisms as well as humans. The 10x Genomic Visium was originally developed for only fresh frozen tissue sections. Initially, this hampered its use to dissect human disease using FFPE patient samples, the standard tissue format in clinical laboratory archives. To overcome this limitation, 10x Genomics developed a FFPE-compatible protocol which uses gene-specific probes that are ligated together in situ in the tissue section using the target mRNA as the template (RNA-templated ligation). The ligated probes are then released from the tissue by permeabilization, diffused from the tissue, and bound to the barcoded capture oligonucleotides printed onto a manufactured slide. Following capture, the probes are extended to incorporate the spatial barcode and then amplified to generate the sequencing library. RNA-templated ligation improves target specificity but incorporates two enzymatic steps prior to library construction that may decrease sensitivity and linearity of response. Conversely, the exquisite sequence specificity required at the point of ligation of bound probes in situ means that probes can be designed that can discriminate between single-nucleotide variants encoded in mRNAs. Both the original and Visium for FFPE protocols use the same barcoded spot array for encoding spatial position of captured mRNAs/probes. We note that the standard clinical workflow for evaluation of kidney biopsies in most medical centers includes a portion of tissue that is processed as frozen material for immunofluorescence microscopy. However, these tissues are typically stabilized in Michel's transport medium, which does not fix tissue. Extended storage of tissue in Michel's medium could result in RNA degradation, which is why Michel's transport medium is not recommended for RNA detection assays such as RNA-FISH. Therefore, clinically sourced frozen kidney biopsy tissues could be made available for spatial transcriptomic evaluation using the original 10x Visium workflow, but without rapid processing after procurement, reduction in RNA quality will impede interpretability of the resulting data.

By contrast, the Nanostring GeoMx DSP uses gene-specific probes that are hybridized to tissue sections. Using a precisely focused UV laser, barcodes that are attached to gene-specific probes are released via cleavage of a photocleavable linker. The released barcodes are captured and converted into a sequencing library. In this approach, spatial information is encoded by user-defined ROI selection. The protocol requires the upfront synthesis of expensive gene-specific probe pools. Whole transcriptome probe pools are commercially available for mouse and human, as well as a streamlined 1,962-target gene panel for canine tissues. In order to study tissues from other model organisms such as pig and zebrafish, bulk synthesis and quality control of custom probes need

Smith/Prince/MacDonald/Bammler/
Akilesh

Table 1. Comparison between GeoMx DSP and 10x Visium portfolio

	Nanostring GeoMx	10x Visium (for frozen tissues)	10x Visium (FFPE)	10x Visium HD
Plex RNA[1]	Up to whole transcriptome (>18,000 genes)	Whole transcriptome (>18,000 genes)	Whole transcriptome (>18,000 genes)	Whole transcriptome (>18,000 genes)
Resolution, μm^2	Variable, dependent on ROI size	55-μm-diameter spots	55-μm-diameter spots	2-μm capture tiles
Resolution (cells)	50–100	10–20	10–20	Single-cell
Analyte detection strategy	Gene-specific probes, barcoded oligos are released by UV light	Poly-A capture and cDNA conversion	Gene-specific probes, in situ ligation (RNA-templated ligation), capture, and barcode addition	Gene-specific probes, in situ ligation (RNA-templated ligation), capture, and barcode addition
Species compatibility	Human, mouse, dog	Any species	Human, mouse	Human, mouse
Ability to use standard microscope slides[3]	Yes	Yes, with CytAssist to transfer tissue onto the assay slide	Yes, with CytAssist to transfer tissue onto the assay slide	Requires CytAssist to transfer tissue onto the assay slide
Selection strategy	User-defined ROI	Fixed grid of capture spots	Fixed grid of capture spots	Fixed grid of capture squares
% of tissue area that is captured	Variable, depends on total ROI area	~28	~28	~100
Tissue	FFPE, fresh frozen	Fresh frozen tissue	FFPE (or fresh frozen tissue)	FFPE (or fresh frozen tissue)
Dedicated instrument	Yes	No	No (recommended with CytAssist)	No (requires CytAssist)
Specialized slides	No	Yes	Yes	Yes
Reagent costs[4]	USD 8,165	USD 19,850	USD 25,725	USD 44,800
Library preparation reagents[5]	USD 1,920	USD 160	USD 160	USD 160
Sequencing cost[6]	USD 2,300	USD 2,300	USD 2,300	USD 2,300
Total cost (16 biopsies)[7]	USD 12,385	USD 22,310	USD 28,315	USD 47,260
Cost/biopsy[7]	USD 774	USD 1,394	USD 1,762	USD 2,954

[1]GeoMx offers panel probes that range from a focused set of ~2,000 genes to whole transcriptome (~18,000), as well as the ability to custom design probes. Visium for frozen tissues relies on sequencing of captured RNA for the whole transcriptome. Visium for FFPE uses gene-specific probes followed by amplification and capture. [2]The minimal diameter for an ROI for GeoMx is determined by the cellularity and requires >20 cells and usually >100 cells; 100 μm diameter is an approximate minimal size that can be interrogated with this technology. Visium Gene Expression uses 55-μm spots that are centered 100 μm apart. See Figure 2 for additional information about resolution. [3]The CytAssist instrument can facilitate transfer of bound probes to the detection slide for 10x Visium assays. It is required for the Visium HD workflow. [4]All costs are stated in US dollars (USD). Reagent costs for Nanostring include Whole Transcriptome Atlas (WTA) probes and running buffers. In GeoMx experiments, it is possible to fit 4 biopsies onto a standard slide for the experiment. The WTA probes provided are sufficient for 4 such slides (16 biopsies). For the 10x systems, the cost for 16 capture frames (4/slide) and reagents is shown since each biopsy will need to be applied to a separate 6.5 × 6.5-mm capture frame. [5]For Nanostring, library preparation reagents are indicated for 192 ROI (12 ROI/biopsy). For Visium, each capture frame requires one library preparation kit. [6]Sequencing costs are estimated as follows: for Nanostring, with 192 ROI × 25,000 μm^2/ROI, this will require 960 × 10^{6} read pairs for readout. For Visium capture frames, from KPMP's Visium Atlas, approximately 20% of the capture frame area is covered in most biopsy tissues applied to the capture frames. The recommended sequencing depth depends on the number of capture frames in the experiment and the percent of the frame covered by tissue. For these experiments, this works out to be 16 biopsies ×20% tissue coverage × 275 × 10^{6} read pairs/capture frame = 880 × 10^{6} read

pairs. We have shown the list price of an Illumina NovaSeq 6000 SP 100-cycle Flow Cell Kit (1.3×10^9 read pairs output) which will suffice for all experiments as outlined. [7]Total cost and cost/biopsy listed in this table only reflect reagents and consumable costs. They do not include additional fees such as taxes, shipping and handling fees, histology service fees, labor costs/overhead for spatial profiling core facilities and overhead for sequencing. Some reagents are bundled together in packs, and only a portion of those materials may be used for the above experiments. Even though the companies require purchase of the entire reagent pack, we have only shown the proportional reagent cost applicable to this experiment. In total, we estimate that these overheads may add an additional 20–25% to the costs shown.

to be performed which require an expensive upfront investment. Alternatively, by leveraging sequence homology of target genes, commercially available probe sets can be applied to the model organism's tissue with the understanding that not all genes may be adequately measured [30]. An advantage of the probe-based approach is that the Nanostring GeoMx DSP is tolerant of mRNA degradation that is frequently encountered in FFPE tissues. Consequently, the Nanostring GeoMx DSP generates high-quality data on both fresh frozen and FFPE tissue sections. Degradation of mRNA impaired the ability of the original 10x Visium to capture full-length poly-adenylated transcripts from FFPE tissues, which in turn spurred development of the RNA-templated ligation protocol. However, as a probe-based strategy, the Visium for FFPE protocol suffers from the same species restriction as GeoMx DSP, with probe sets currently available only for human and mouse tissues (Table 1).

Even beyond the differences noted above, the biggest consideration in choosing between these platforms is the strategy by which features are selected for gene expression quantification. As noted previously, the original 10x Genomics Visium platform provides a map of gene expression that consists of a matrix of nonoverlapping spots of 55 μm in diameter with an interspot pitch (center-to-center distance) of 100 μm. The tissues need to be applied to a specialized slide within a capture frame containing this barcoded spot matrix in both the original (fresh frozen) and Visium for FFPE workflows. While often presented as covering the entire tissue surface, in reality, the gaps between spots means that only ~28% of the capture frame area is available for expression profiling. This prompted 10x Genomics to develop an even higher density capture array termed Visium HD. In this updated capture frame, the entire surface area is covered by 2×2-μm capture tiles with spatial barcodes with no gaps between the capture tiles. Using the same 6.5-mm square capture frame, this increases the spot density from ~5,000 in the original Visium to >11 million in Visium HD. The higher density of capture tiles is more expensive and requires more analysis time but provides single-cell level resolution data (Table 1). The Visium HD system has just been released commercially and is not yet widely available. It also requires purchase of a separate CytAssist instrument to properly place tissue sections within the capture frame. The geographic gene expression profiles generated by the Visium platforms are extremely powerful in deciphering gene expression patterns and gradients across an entire tissue section (see the Opportunities section below). However, at least for the more widely available and affordable Visium platform, since the spot size is fixed at 55 μm and there is no control over how a tissue section is placed on the capture matrix, it is not possible to specifically capture the expression profile of a defined structure such as a glomerulus. This is not an issue with the Visium HD platform which generates single-cell resolution data, from which a glomerulus can be computationally defined based on its constituent cells.

By contrast, the Nanostring GeoMx DSP uses a targeted ROI selection strategy, which allows precise capture of the gene expression profile of histologic structures such as glomeruli. ROIs can be drawn in any freeform shape to conform to the histologic structure of interest, so long as they contain 50–100 cells in order to generate a reliable expression signature. Portions of a glomerulus with a discernible lesion such as crescents or segmental scars could be profiled separately from the remainder of the glomerulus, in effect creating a sub-glomerular resolution assay. This may be particularly effective for glomerular diseases which may affect only a fraction of the total glomeruli in a biopsy sample. In addition, since fluorescently labeled antibodies are included in the assay to outline tissue morphology, these can be used to segment discontinuous cells (e.g., infiltrating leukocytes labeled with CD45). However, the downside of ROI-based approach is that if a map of gene expression across the entire tissue section is desired, then the associated sequencing requirements would be cost-prohibitive. Therefore, with ROI-based selection, the entire tissue cannot reasonably be sampled and there is subjectivity introduced in manual selection of ROIs (also see the Challenges section below). The difference in feature selection between these two
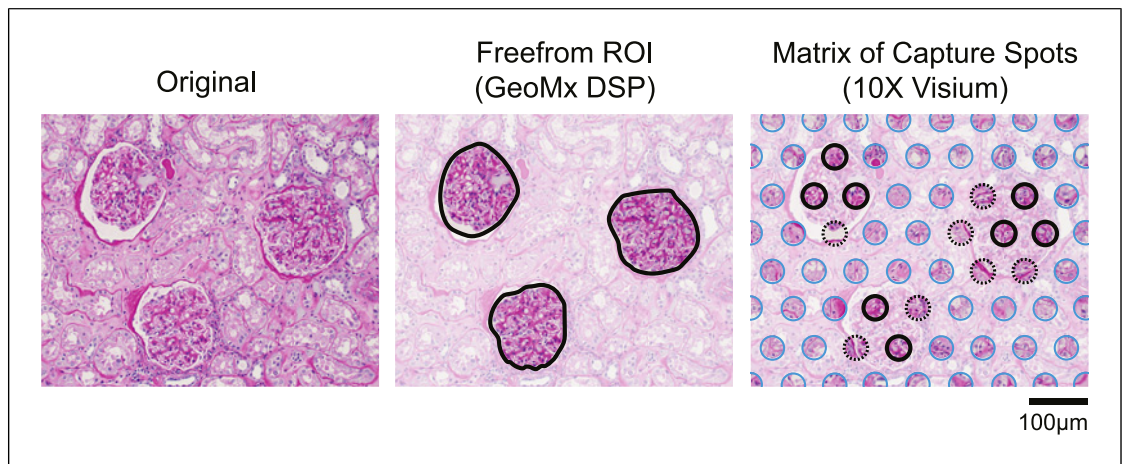
| Original | Freefrom ROI (GeoMx DSP) | Matrix of Capture Spots (10X Visium) |

100μm

Fig. 2. Differences in regions profiled in the two most widely utilized spatial transcriptomics platforms. The left panel shows a section of PAS-stained renal cortex with 3 glomeruli surrounded by tubular parenchyma. The middle panel shows a hypothetical representation of the same section with overlaid freeform ROIs, as would be seen using the GeoMx DSP platform. The freeform ROIs can be drawn to collect probes from any given region within the dimensions of ~ 5–650 μm, allowing precise outlining of glomeruli. As shown, the ROIs have a diameter of ~125 μm. The transcriptomic signature is generated only from the selected ROIs. In this representation, the gene expression signature of the tubules surrounding the glomeruli would not be obtained. The right panel shows an overlap of capture spots that are used to create a geo-graphic gene expression profile over a tissue section using the 10x Visium platform. Each spot is 55 μm in diameter, and the distance between two adjacent spot centers is 100 μm. The tissue is overlaid on the capture array, and a transcriptomic signature is generated from each spot. If glomerular diseases are of interest, then the capture spot may be present entirely within glomeruli (black heavy outline), tubular parenchyma (blue), or straddle glomeruli and tubules (dotted black outline). While individual glomeruli cannot be precisely selected using this approach, there is no bias associated with ROI selection and the entire tissue, including the tubular parenchyma can be profiled at the same time. Of note, both GeoMx DSP and Visium capture a composite signature from 10's–100's of cells. PAS, periodic acid-Schiff.

systems is illustrated using a section of human kidney tissue in Figure 2. The expression profiles generated by GeoMx DSP with user-defined ROIs and Visium using 55-μm capture spots represent a composite signature of multiple cells. Therefore, orthogonally generated single-cell RNA-seq data are often used to computationally deconvolve the relative cellular composition of the expression profiles generated by these spatial methods [31, 32]. Balancing the strengths and weaknesses of these platforms is needed to choose the best approach to answering the investigator's biological question. In our opinion, for studying glomerular disease from clinically sourced FFPE human kidney biopsies, the ability to precisely select individual glomeruli and correlate their expression profiles with histology gives the advantage to the Nanostring GeoMx DSP platform. Analysis of glomerular ROIs in GeoMx DSP experiments is straight-forward, but preselection of capture spots that are enriched for glomerular transcripts may be necessary in 55-μm spot-based Visium experiments (Fig. 2). However, as it will be shown below, the 10x Visium platform may be better suited to answer biological questions at the level of the entire tissue section.

Insights into Kidney Disease Gleaned from Spatial Transcriptomics and Opportunities for Clinical Translation

There has been rapid adoption of spatial tran-scriptomic platforms to study kidney development and disease in patient samples and animal models. The KPMP, HuBMAP, and other groups have used the 10x Genomics Visium system to generate reference atlases of human kidney from nephrectomy specimens and kidney biopsies [1, 2, 33]. These atlases define the spatial and functional organization of the kidney, altered/injured epithelial cells states and their niches, as well as the associated responses by immune cells. Additional studies using 10x Genomics Visium on human kidney tissues have provided insights into kidney development [34], angiogenesis, and inflammation in diabetic kidney disease [35, 36], roles for innate immune cells in allograft rejection [37], epithelial cell-immune cell crosstalk in acute kidney injury [38], and remodeling mechanisms in the medulla in response to nephrolithiasis [39]. Investigators have also applied this powerful technology to study mouse models of ischemia reperfusion kidney injury [38,

40, 41] and chronic kidney disease induced by aristolochic acid [42]. One exemplary study of murine acute kidney injury demonstrated spatial and temporal heterogeneity in transcription programs as well as substantial sex-specific differences [43]. The species agnostic nature of the poly(A) mRNA capture has been leveraged to apply spatial transcriptomic analysis to rat models of losartan treatment and nephrolithiasis [44, 45]. The release of the FFPE-compatible Visium protocol has enabled study on archival FFPE tissue samples. For the study of glomerular disease, the inability to precisely place ROI over glomeruli has proved challenging, though these studies were able to somewhat work around this limitation by using in silico cellular decomposition approaches and selecting glomerulus-enriched ROIs by their expression of glomerular cell marker genes. Conversely, the unbiased placement of ROIs over the tissue section and whole-tissue coverage enabled spatial insights and neighborhood analysis that would be harder to achieve with a more targeted ROI selection scheme (see next).

The FFPE compatibility of the Nanostring GeoMx DSP has seen its application to clinically sourced kidney biopsies and tissues. For example, a large study of COVID-19 autopsies demonstrated regional differences in inflammatory responses in multiple organs, including the lung and kidney [46]. This study also demonstrated two distinguishing features of the DSP. First, during ROI selections, the authors used fluorescently labeled antibodies for pan-cytokeratin (panCK) to mask the image and capture transcriptional information from panCK+ and panCK− regions of tissues. Second, using the spike in probes, the authors were able to interrogate the tissue localization of SARS-CoV-2 viral RNAs in parallel with tissue gene expression profiles. They concluded that viral RNAs were not detected at significant levels outside the lung and airways, a finding that we confirmed using the same approach in kidney biopsies [47]. Though SARS-CoV-2 genomic RNA is polyadenylated [48], not all viruses produced poly(A) RNA genomes, and these molecules as well as subsets of cellular RNAs (microRNAs, enhancer RNAs) would be missed in poly(A)-based capture strategies such as the Visium for fresh frozen tissue protocol. The first clinically sourced biopsy-based DSP study of kidney disease was performed in an allograft biopsy undergoing rejection [49]. That study demonstrated the feasibility of correlating histopathologic features (i.e., Banff scores) with gene expression profiles and spatial localization. Two subsequent studies have explored signatures in pauci-immune complex (ANCA-associated) glomerulonephritis [50, 51]. These studies were able to correlate glomerular histology (e.g., crescentic vs. uninvolved) with gene expression signatures. They were able to demonstrate the involvement of the classical complement pathway in glomerular injury and osteopontin signaling in fibrosis responses. Our own study of collapsing glomerulopathy demonstrated the power of analyzing individual glomerular ROIs using DSP [47]. By annotating collapsing and non-collapsing glomeruli, we were able to demonstrate substantial intra- and inter-patient variability in glomerular transcriptome responses to HIV and SARS-CoV-2 infections. Since each glomerulus was considered individually, our study demonstrated improved sensitivity compared to a prior laser capture microdissection study of collapsing glomerulopathy that needed to pool multiple glomeruli to achieve sufficient signal [52]. Importantly, we showed that glomeruli with similar histologic appearances can have very different transcriptional signatures, illustrating the additional information that can be obtained by adding this "molecular layer" to routine pathologic evaluations. We also showed that findings from DSP could be validated using immunohistochemistry and RNA-ISH, techniques that are readily accessible in pathology laboratories. Integrating scRNA-seq data, we were able to deconvolute the relative cellular contributions in the multicellular glomerular ROIs and identify distinct pathogenic trajectories in collapsing glomerulopathy [53]. These early DSP studies used a focused gene panel of ~1,800 genes, but more recently, a whole transcriptome probe panel has been released and used to study diabetic kidney disease [54]. Leveraging the probes with >85% sequence homology, investigators have recently used the human whole transcriptome probe set to study porcine xenograft rejection [30]. These investigators examined both glomerular and tubulointerstitial ROIs and found that antibody-mediated rejection was more pronounced in glomeruli with influx of monocytes, macrophages, and natural killer cells. Finally, we have recently shown that spatial profiling can be used to validate findings from other -omics technologies in place of traditional techniques such as immunohistochemistry [55].

Taken together, the distinct ROI selection approaches of the Visium and GeoMx DSP platforms have been intersected with other powerful -omics technologies to spatially localize gene expression programs in kidney tissue and reveal novel biological insights and mechanisms. Excitingly, the potential to apply these methods to clinically sourced biopsy tissues promises to introduce spatial molecular diagnostic approaches to kidney biopsy interpretation and improve patient care.

Smith/Prince/MacDonald/Bammler/
Akilesh

Challenges for Clinical Translation of Spatial Transcriptomics Technologies

Several technical and regulatory challenges need to be considered in translating spatial transcriptomics technologies to the clinic. On the technical side, while the manufacturers have released white papers on the rigor and reproducibility of their platforms, independent assessment of their performance and the impact of preanalytic variables must be published in peer-reviewed publications. The ideal study would quantify the contributions of biologic and technical sources of variability to the observed data. Biologic sources of variability include donor differences and tissue histology. Technical sources of variability are myriad and may include preanalytical variables such as formalin fixation time, age of the tissue block, reproducibility of results performed on the same specimen from 1 day to the next, operator-effects, reagent lots, sequencing batch effects, and subjectivity in ROI selection (in the case of GeoMx DSP). It will be necessary to understand these effects in order to deploy spatial transcriptomics as a laboratory-developed test (LDT) and potentially gain Food and Drug Administration (FDA) approval. Also critical to LDT development is the incorporation of benchmarks that are evaluated at regular intervals to ensure that the platform is stable and to ensure comparability and interoperability of data collected at different times. One approach to address these issues is to generate a tissue fiducial that can be sequentially interrogated via spatial transcriptomic profiling at regular intervals (Fig. 3). As an example, a fiducial nephrectomy tissue microarray could incorporate biological variables such as multiple donors and preanalytic variables such as formalin fixation time. In order to preserve RNA quality of this fiducial block for reproducible comparisons over time, it can be stored at −20°C or lower temperatures, which has been shown to preserve nucleic acid integrity [56]. It will also allow for batch correction across sequencing runs, such as with the Bioconductor RUVSeq package [57]. Specifically, the RUVs function in this package can be used to estimate batch-specific effects from repeated runs of the same sample and enable creation of a cumulative database of spatial profiling data. Tissue fiducials could also be shared across institutions for external validation of spatial profiling data generation.

Standardization of ROI selection in DSP experiments could be achieved using artificial intelligence approaches adapted to multiplexed immunofluorescence images [58–60]. When histologic structures within a sample are assumed to be uniformly affected by a disease process (e.g., all glomeruli in minimal change disease), it will be necessary to determine how many glomerular ROIs are needed to accurately capture the disease signature. This is in contrast to diseases in which lesional and non-lesional glomeruli are histologically apparent [47, 50, 51]. Since ROIs in DSP experiments may be of different sizes, once the data are generated, systematic evaluation of normalization methods will also be necessary [61]. While research data analysis incorporates wide-ranging approaches such as differential gene expression, gene ontology and pathway enrichment, cellular decomposition, and disease trajectory/pseudotime analysis, it will be necessary to standardize and distill these findings into clinically meaningful and actionable reports. Publication of consensus best practices will be needed in order to onboard new sites and to ensure reproducibility as has been shown in other fields [62, 63].

The use of a composite gene expression signature has had a long track record of clinical utility in subtyping cancer and predicting response to therapy [64, 65]. With respect to kidney disease, the experience of the molecular microscope diagnostic system (MMDx) is instructive [66]. This assay requires submission of a dedicated 3- to 5-mm core of kidney tissue for whole transcriptome microarray-based gene expression profiling. Since the microarray platform has remained consistent over the ~20-year period of MMDx development, it is possible to integrate prospectively collected samples into a growing database of now almost ~1,700 kidney allograft pathology gene signatures. Numerous studies have compared the nonspatially localized information gleaned from MMDx with traditional pathologic evaluation of the kidney allograft and the Banff scoring scheme [67–70]. With MMDx, test results are returned in 48 h and presented in a two-page report displaying a principal component analysis, placing the submitted sample in the expression space of the assay's database. This permits assignment of scores that describe the individual's risk of various types of rejection, parenchymal injury, infection, and fibrosis. The MMDx results then need to be interpreted as an adjunct to traditional pathologic evaluation of a separate core of biopsy tissue. A short turnaround time, evidence-based design, and simplified reporting of the MMDx scheme would be desirable in any clinical implementation of spatial transcriptomics technology. Notably, the MMDx assay requires a dedicated portion of kidney biopsy tissue and prospective tissue collection, and it took almost 15–20 years to accrue a large database. By modeling effect size and proportion of the population with
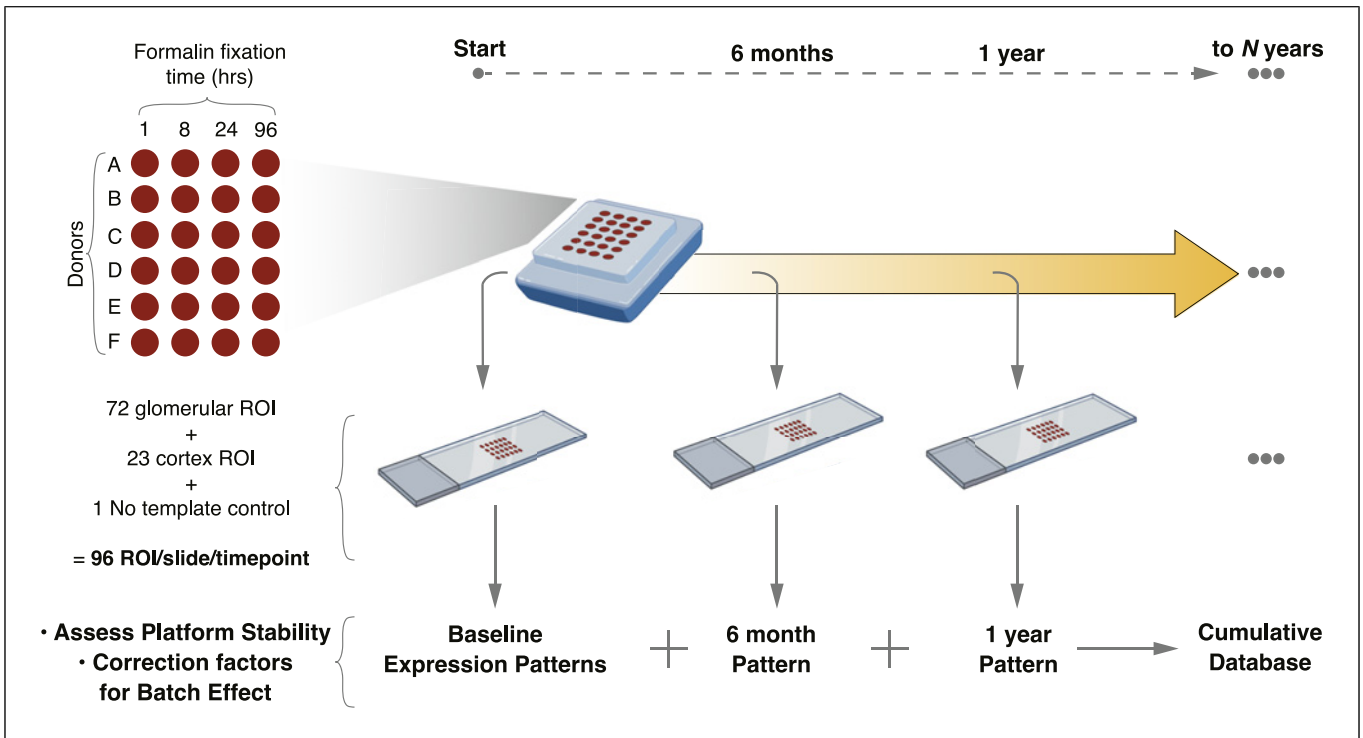
Fig. 3. Tissue fiducials can help benchmark platform stability over time. A tissue microarray block can be constructed using reference tissue obtained from human kidney tissues (e.g., from nephrectomies). Pre-analytic variables such as formalin fixation time and donor variability can be incorporated into individual tissue cores. Sections from this fiducial block can be assessed using spatial profiling methods, and the resulting data can be used to understand platform stability and batch-to-batch variability as well as to study the impact of pre-analytic variables on data quality. To preserve RNA integrity and ensure comparability of results, the fiducial block can be stored at −20°C between experiments. Image created in part using BioRender.com.

Fig. 4. Increasing sample size has a dramatic effect on the power to detect differences. The figure shows power (*y*-axis) for two-group comparisons when varying the percent of the total for one group (*x*-axis) with total sample sizes of 100 and 400 and considering four different effect sizes. Analyses use an alpha of 0.05, assuming 18,000 total tests and adjusting for multiple comparisons with a Bonferroni correction. This analysis does not account for power gains that could be achieved by sampling multiple similar ROIs (e.g., glomeruli) from each patient.

Smith/Prince/MacDonald/Bammler/
Akilesh
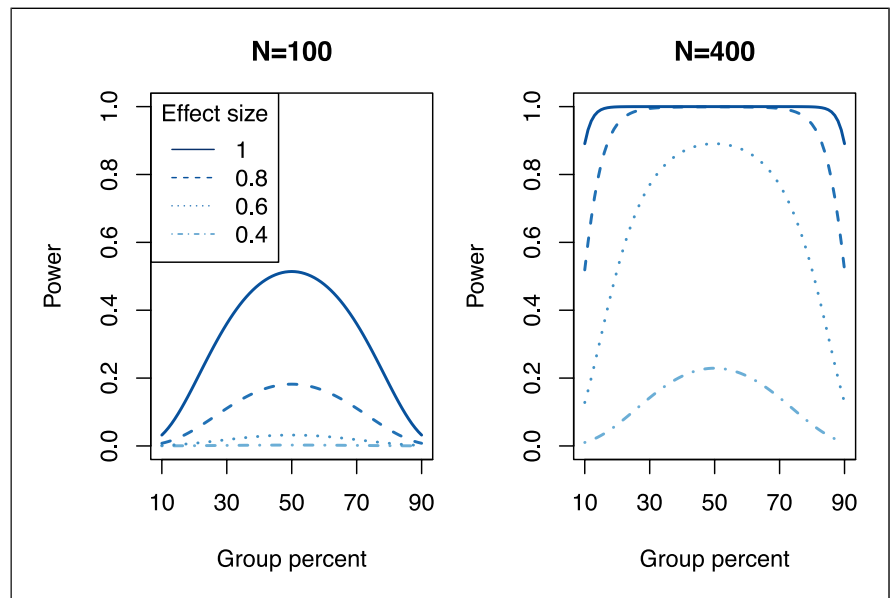
the measured effect, it becomes apparent that large cohorts of >400 patients are needed to achieve sufficient power to identify subgroups and subtle in-group variation (Fig. 4). The particulars of spatial transcriptomics experiments may impact these power calculations. For example, power may be gained by sampling multiple similar structures (e.g., glomeruli) from an individual, using a focused set of glomerular disease-relevant genes to reduce multiple testing penalty and by using less stringent multiple testing correction approaches such as the false discovery rate. In a conceptually similar approach, manual or laser capture microdissection approaches have also been applied by the NEPTUNE consortium to study glomerular disease in 200+ patients [71]. Focusing only on two types of glomerular disease improved the study power, and these investigators identified novel pathways such as tumor necrosis factor (TNF) activation, as playing a key role in progression of a subset of patients with FSGS and MCD. Independently, we have been able to validate findings from that study in a DSP experiment performed on 14 patients with MCD, but in our case, we were able to use a single 5-μm section of archival FFPE tissue (data not shown). Therefore, the ability to use archival FFPE material for spatial transcriptomics technologies such as GeoMx DSP is a powerful advantage since it will enable groups to collect data on sufficient numbers of patients to achieve power and clinical utility without the need for prospective tissue collection/microdissection.

These exciting possibilities must be balanced by practical challenges. For example, the high cost of spatial transcriptomics instruments, service contracts, and reagents may limit their widespread deployment. They are also tempered by the fact that clinical biopsy-based studies are necessarily impacted by selection of a subset of patients with indication for biopsy, limited sampling of tissue, and assessment at a single timepoint of disease progression. Assays such as MMDx require extensive quality control and specialized expertise and are therefore performed at a centralized laboratory. A similar model may apply to any spatial transcriptomics assay validated for clinical use. Importantly, it has yet to be systematically demonstrated that the availability of spatial transcriptomic profiling data can positively impact clinical decision making, though anecdotes of such are emerging from KPMP studies [35, 72]. A new initiative termed NEPTUNE Match integrates clinical, biomarker, and laboratory data (including several -omics technologies) to identify glomerular disease pathways that may be active in individual patients [73]. This information is then used to guide these individuals

toward clinical trials that may be best positioned to address their underlying glomerular disease mechanism. From this perspective, our ability to reproduce MCD biopsy findings from the NEPTUNE cohort suggests that spatial transcriptomics can be integrated into the NEPTUNE Match workflow. The analogous concept of a "molecular tumor board" and multimodal data integration has substantially precedent in the oncology arena, and it will be exciting to see a similar approach being applied to help patients with glomerular diseases. Alternatively, the best performing genes (or their protein products) identified from spatial profiling studies could be validated and rapidly deployed as lower cost ancillary LDTs in the form of routine immunohistochemistry or RNA-ISH assays or even quantitative RT-PCR assays performed on existing FFPE tissues [74]. Therefore, rather than spatial profiling itself being deployed as a clinical tool, the more pragmatic and expedient solution may be to use it for discovery and then leverage existing laboratory methodologies to apply the lessons learned. Focused gene panels relevant to glomerular disease can be designed for the GeoMx DSP platform, which combined with glomerular-focused ROI selection, would increase throughput, decrease sequencing costs, and increase power to detect significant expression changes. These solutions have different developmental timelines associated with them and could coexist to accelerate the application of spatial profiling technologies in both discovery and clinical modes.

We also need to consider regulatory hurdles and strategic uncertainties that exist in translating a new technology such as spatial transcriptomics to commercial deployment in the healthcare setting. Despite its long track record of utility and validation, MMDx tests have not yet received approval from the FDA. Therefore, as an LDT, MMDx tests have limited reimbursement options which may have impacted their widespread clinical utilization. By contrast, another molecular biomarker, donor-derived cell-free DNA, has seen widespread adoption for kidney transplant rejection screening following FDA approval. Medicare and other health insurance payors in the USA have reimbursed for these tests (~USD 3,000/assay), though their price-point may still be too high for routine screening in other countries such as Canada, where a screening test needs to be <USD 300 for use in their health system (Dr. Paul Keown and others, University of British Columbia, personal communication). The importance of FDA approval is also underscored by the agency's continuous push to bring tighter regulatory oversight over LDTs [75]. In this new

landscape, it may be even more difficult to deploy LDTs using newer technologies such as spatial transcriptomics. Finally, there is ongoing litigation among 10x Genomics, Nanostring, and Vizgen. As a result of early decisions and financial penalties (which are being appealed), Nanostring filed for Chapter 11 protections on February 4, 2024, and is undergoing financial restructuring. In a turn of events, on February 26, 2024, the European Unified Patent Court (UPC) of Appeals revoked a preliminary injunction and ruled in favor of Nanostring. Besides the technical differences among the platforms that we have outlined above, these ongoing legal challenges introduce uncertainty into spatial transcriptomics technology landscape.

Emerging Technologies

Several new spatial formats that achieve single cell resolution have been recently released and include the previously mentioned 10x Visium HD which uses barcoded capture of gene-specific probes released from tissue followed by a sequencing-based readout. Other newly commercialized technologies rely on serial hybridization and detection of fluorescent probes in situ in tissue sections and use microscopy as a readout. The two most widely distributed of these systems are the Xenium by 10x Genomics and the CosMx Spatial Molecular Imager (SMI) by Nanostring, though the MERSCOPE system by Vizgen is also gradually increasing in availability. These technologies offer higher spatial resolution, even to the subcellular level, and can simultaneously measure and localize an impressive number of transcripts: 100's–1,000's of genes for Xenium, ~500 genes for MERSCOPE, and up to 6,000 genes for CosMx. Nanostring has also reported feasibility of whole transcriptome level of interrogation at single-cell resolution for CosMx, though those reagents are not commercially available at this writing. As imaging-based technologies, these instruments rely on delineation of cell boundaries to assign detected transcripts to cells. This process, which is termed segmentation, requires reliable labeling of cell membranes, cytoplasm, and nuclei; high fidelity optics within the microscope; and powerful algorithms to define cellular boundaries. Though imprecise, segmentation approaches are continuously being improved with assistance from artificial intelligence. Powerfully, the cellular resolution transcriptome data generated by these platforms allow researchers to ask additional questions about cellular neighborhoods and the spatial organization of cells, including receptor-ligand interactions using analysis tools such as CellNeighborEx and COMMOT [76, 77]. The single cell spatial analysis also theoretically allows for the identification and assaying of cells that are challenging to dissociate and study using single cell and single nucleus technologies. Similarly, spatial heterogeneity in gene expression, which may contribute to disease phenotype and response to therapy, could be revealed with these higher resolution technologies. These single cell spatial technologies can have extended run times to collect all the data, which tend to be proportional to the number of probes quantified and the area that is interrogated. In addition, the sensitivity of gene expression and the dynamic range are not well established for these platforms. Finally, the increased cost of these technologies, which are even greater than those for GeoMx and Visium listed in Table 1, may be a barrier to their adoption.

Perspectives

The explosion of spatial technologies and their compatibility with FFPE tissues have opened up the vast archive of clinical specimens to interrogation. These technologies are ripe to use in research settings to gain novel insights into biology through spatial definition of gene and protein expression and even protein modifications. The discoveries made could lead to novel biomarkers to help diagnose diseases and guide treatment. In addition, higher plex platforms of biomarkers may become useful tools in the setting of clinical trials and advanced diseases to personalize therapeutic choices and options based on molecular profiles that can predict response to therapy. The ability to perform higher plex analysis on FFPE tissues is in itself valuable due to the limited nature of core biopsies and the need to use this tissue judiciously.

Conflict of Interest Statement

Funding Sources

through the University of Washington, received support from the NIH, the Doris Duke Charitable Foundation, and the National Palliative Care Research Center unrelated to this work.

Author Contributions

Kelly D. Smith, David K. Prince, James W. MacDonald, Theo K. Bammler, and Shreeram Akilesh made substantial contributions to the analysis and interpretation of data. Kelly D. Smith and Shreeram Akilesh contributed to the conception the work and drafting of the initial manuscript. Shreeram Akilesh used the artificial intelligence-based image generator DALL-E2 to create panels in Figure 1 based on his concept. Kelly D. Smith, David K. Prince, James W. MacDonald, Theo K. Bammler, and Shreeram Akilesh reviewed the manuscript for accuracy of intellectual content and approved the final version of the manuscript. Kelly D. Smith, David K. Prince, James W. MacDonald, Theo K. Bammler, and Shreeram Akilesh agree to be accountable for all aspects of the work in ensuring that questions related to the accuracy or integrity of any part of the work are appropriately investigated and resolved.

References

1 HuBMAP Consortium. The human body at cellular resolution: the NIH Human Biomolecular Atlas Program. Nature. 2019; 574(7777):187–92. doi: 10.1038/s41586-019-1629-x.

2 Lake BB, Menon R, Winfree S, Hu Q, Melo Ferreira R, Kalhor K, et al. An atlas of healthy and injured cell states and niches in the human kidney. Nature. 2023;619(7970): 585–94. doi: 10.1038/s41586-023-05769-3.

3 Hinze C, Karaiskos N, Boltengagen A, Walentin K, Redo K, Himmerkus N, et al. Kidney single-cell transcriptomes predict spatial corticomedullary gene expression and tissue osmolality gradients. J Am Soc Nephrol. 2021;32(2):291–306. doi: 10.1681/ASN.2020070930.

4 Lindstrom NO, Sealfon R, Chen X, Parvez RK, Ransick A, De Sena Brandine G, et al. Spatial transcriptional mapping of the human nephrogenic program. Dev Cell. 2021;56(16): 2381–98.e6. doi: 10.1016/j.devcel.2021.07.017.

5 Nitzan M, Karaiskos N, Friedman N, Rajewsky N. Gene expression cartography. Nature. 2019;576(7785):132–7. doi: 10.1038/s41586-019-1773-3.

6 Qian J, Liao J, Liu Z, Chi Y, Fang Y, Zheng Y, et al. Reconstruction of the cell pseudo-space from single-cell RNA sequencing data with scSpace. Nat Commun. 2023;14(1):2484. doi: 10.1038/s41467-023-38121-4.

7 Femino AM, Fay FS, Fogarty K, Singer RH. Visualization of single RNA transcripts in situ. Science. 1998;280(5363):585–90. doi: 10.1126/science.280.5363.585.

8 Raj A, van den Bogaard P, Rifkin SA, van Oudenaarden A, Tyagi S. Imaging individual mRNA molecules using multiple singly labeled probes. Nat Methods. 2008;5(10): 877–9. doi: 10.1038/nmeth.1253.

9 Battich N, Stoeger T, Pelkmans L. Image-based transcriptomics in thousands of single human cells at single-molecule resolution. Nat Methods. 2013;10(11):1127–33. doi: 10.1038/nmeth.2657.

10 Kishi JY, Lapan SW, Beliveau BJ, West ER, Zhu A, Sasaki HM, et al. SABER amplifies FISH: enhanced multiplexed imaging of RNA and DNA in cells and tissues. Nat Methods. 2019;16(6):533–44. doi: 10.1038/s41592-019-0404-0.

11 Lee JH, Daugharthy ER, Scheiman J, Kalhor R, Yang JL, Ferrante TC, et al. Highly multiplexed subcellular RNA sequencing in situ. Science. 2014;343(6177):1360–3. doi: 10.1126/science.1250212.

12 Chen KH, Boettiger AN, Moffitt JR, Wang S, Zhuang X. RNA imaging. Spatially resolved, highly multiplexed RNA profiling in single cells. Science. 2015;348(6233):aaa6090. doi: 10.1126/science.aaa6090.

13 Moffitt JR, Hao J, Wang G, Chen KH, Babcock HP, Zhuang X. High-throughput single-cell gene-expression profiling with multiplexed error-robust fluorescence in situ hybridization. Proc Natl Acad Sci USA. 2016; 113(39):11046–51. doi: 10.1073/pnas.1612826113.

14 Moffitt JR, Hao J, Bambah-Mukku D, Lu T, Dulac C, Zhuang X. High-performance multiplexed fluorescence in situ hybridization in culture and tissue with matrix imprinting and clearing. Proc Natl Acad Sci USA. 2016;113(50):14456–61. doi: 10.1073/pnas.1617699113.

15 Moffitt JR, Bambah-Mukku D, Eichhorn SW, Vaughn E, Shekhar K, Perez JD, et al. Molecular, spatial, and functional single-cell profiling of the hypothalamic preoptic region. Science. 2018;362(6416):eaau5324. doi: 10.1126/science.aau5324.

16 Xia C, Babcock HP, Moffitt JR, Zhuang X. Multiplexed detection of RNA using MERFISH and branched DNA amplification. Sci Rep. 2019;9(1):7721. doi: 10.1038/s41598-019-43943-8.

17 Xia C, Fan J, Emanuel G, Hao J, Zhuang X. Spatial transcriptome profiling by MERFISH reveals subcellular RNA compartmentalization and cell cycle-dependent gene expression. Proc Natl Acad Sci USA. 2019;116(39): 19490–9. doi: 10.1073/pnas.1912459116.

18 Su JH, Zheng P, Kinrot SS, Bintu B, Zhuang X. Genome-scale imaging of the 3D organization and transcriptional activity of chromatin. Cell. 2020;182(6):1641–59.e26. doi: 10.1016/j.cell.2020.07.032.

19 Lee JH, Daugharthy ER, Scheiman J, Kalhor R, Ferrante TC, Terry R, et al. Fluorescent in situ sequencing (FISSEQ) of RNA for gene expression profiling in intact cells and tissues. Nat Protoc. 2015;10(3):442–58. doi: 10.1038/nprot.2014.191.

20 Merritt CR, Ong GT, Church SE, Barker K, Danaher P, Geiss G, et al. Multiplex digital spatial profiling of proteins and RNA in fixed tissue. Nat Biotechnol. 2020;38(5):586–99. doi: 10.1038/s41587-020-0472-9.

21 Asp M, Giacomello S, Larsson L, Wu C, Fürth D, Qian X, et al. A spatiotemporal organ-wide gene expression and cell atlas of the developing human heart. Cell. 2019;179(7): 1647–60.e19. doi: 10.1016/j.cell.2019.11.025.

22 Stahl PL, Salmen F, Vickovic S, Lundmark A, Navarro JF, Magnusson J, et al. Visualization and analysis of gene expression in tissue sections by spatial transcriptomics. Science. 2016;353(6294):78–82. doi: 10.1126/science.aaf2403.

23 Salmen F, Stahl PL, Mollbrink A, Navarro JF, Vickovic S, Frisén J, et al. Barcoded solid-phase RNA capture for Spatial Transcriptomics profiling in mammalian tissue sections. Nat Protoc. 2018;13(11):2501–34. doi: 10.1038/s41596-018-0045-2.

24 Stickels RR, Murray E, Kumar P, Li J, Marshall JL, Di Bella DJ, et al. Highly sensitive spatial transcriptomics at near-cellular resolution with Slide-seqV2. Nat Biotechnol. 2021;39(3): 313–9. doi: 10.1038/s41587-020-0739-1.

25 Vickovic S, Eraslan G, Salmen F, Klughammer J, Stenbeck L, Schapiro D, et al. High-definition spatial transcriptomics for in situ tissue profiling. Nat Methods. 2019;16(10): 987–90. doi: 10.1038/s41592-019-0548-y.

26 Chen A, Liao S, Cheng M, Ma K, Wu L, Lai Y, et al. Spatiotemporal transcriptomic atlas of mouse organogenesis using DNA nanoball-patterned arrays. Cell. 2022;185(10): 1777–92.e21. doi: 10.1016/j.cell.2022.04.003.

27 Liu C, Li R, Li Y, Lin X, Zhao K, Liu Q, et al. Spatiotemporal mapping of gene expression landscapes and developmental trajectories during zebrafish embryogenesis. Dev Cell. 2022;57(10):1284–98.e5. doi: 10.1016/j.devcel.2022.04.009.

28 Wang M, Hu Q, Lv T, Wang Y, Lan Q, Xiang R, et al. High-resolution 3D spatiotemporal transcriptomic maps of developing Drosophila embryos and larvae. Dev Cell. 2022; 57(10):1271–83.e4. doi: 10.1016/j.devcel. 2022.04.006.

29 Xia K, Sun HX, Li J, Li J, Zhao Y, Chen L, et al. The single-cell stereo-seq reveals region-specific cell subtypes and transcriptome profiling in Arabidopsis leaves. Dev Cell. 2022;57(10):1299–310.e4. doi: 10.1016/j. devcel.2022.04.011.

30 Loupy A, Goutaudier V, Giarraputo A, Mezine F, Morgand E, Robin B, et al. Immune response after pig-to-human kidney xenotransplantation: a multimodal phenotyping study. Lancet. 2023;402(10408):1158–69. doi: 10.1016/S0140-6736(23)01349-1.

31 Danaher P, Kim Y, Nelson B, Griswold M, Yang Z, Piazza E, et al. Advances in mixed cell deconvolution enable quantification of cell types in spatial transcriptomic data. Nat Commun. 2022;13(1):385. doi: 10.1038/ s41467-022-28020-5.

32 Elosua-Bayes M, Nieto P, Mereu E, Gut I, Heyn H. SPOTlight: seeded NMF regression to deconvolute spatial transcriptomics spots with single-cell transcriptomes. Nucleic Acids Res. 2021;49(9):e50. doi: 10.1093/nar/ gkab043.

33 Raghubar AM, Pham DT, Tan X, Grice LF, Crawford J, Lam PY, et al. Spatially resolved transcriptomes of mammalian kidneys illustrate the molecular complexity and interactions of functional nephron segments. Front Med. 2022;9:873923. doi: 10.3389/ fmed.2022.873923.

34 Wu H, Liu F, Shangguan Y, Yang Y, Shi W, Hu W, et al. Integrating spatial transcriptomics with single-cell transcriptomics reveals a spatiotemporal gene landscape of the human developing kidney. Cell Biosci. 2022;12(1):80. doi: 10.1186/s13578-022-00801-x.

35 Ferkowicz MJ, Verma A, Barwinska D, Ferreira RM, Henderson JM, Kirkpatrick M, et al. Molecular signatures of glomerular neovascularization in a patient with diabetic kidney disease. Clin J Am Soc Nephrol. 2023;19(2):266–75. doi: 10.2215/CJN.0000000000000276.

36 Chen D, Shao M, Song Y, Ren G, Guo F, Fan X, et al. Single-cell RNA-seq with spatial transcriptomics to create an atlas of human diabetic kidney disease. FASEB J. 2023;37(6):e22938. doi: 10.1096/fj.202202013RR.

37 Lamarthee B, Callemeyn J, Van Herck Y, Antoranz A, Anglicheau D, Boada P, et al. Transcriptional and spatial profiling of the kidney allograft unravels a central role for FcγRIII+ innate immune cells in rejection. Nat Commun. 2023;14(1):4359. doi: 10.1038/ s41467-023-39859-7.

38 Melo Ferreira R, Sabo AR, Winfree S, Collins KS, Janosevic D, Gulbronson CJ, et al. Integration of spatial and single-cell transcriptomics localizes epithelial cell-immune cross-talk in kidney injury. JCI Insight. 2021;

6(12):e147703. doi: 10.1172/jci.insight. 147703.

39 Canela VH, Bowen WS, Ferreira RM, Syed F, Lingeman JE, Sabo AR, et al. A spatially anchored transcriptomic atlas of the human kidney papilla identifies significant immune injury in patients with stone disease. Nat Commun. 2023;14(1):4140. doi: 10.1038/ s41467-023-38975-8.

40 Cheung MD, Erman EN, Moore KH, Lever JM, Li Z, LaFontaine JR, et al. Resident macrophage subpopulations occupy distinct microenvironments in the kidney. JCI Insight. 2022;7(20):e161078. doi: 10.1172/jci. insight.161078.

41 Li JSY, Robertson H, Trinh K, Raghubar AM, Nguyen Q, Matigian N, et al. Tolerogenic dendritic cells protect against acute kidney injury. Kidney Int. 2023;104(3):492–507. doi: 10.1016/j.kint.2023.05.008.

42 Kayhan M, Vouillamoz J, Rodriguez DG, Bugarski M, Mitamura Y, Gschwend J, et al. Intrinsic TGF-β signaling attenuates proximal tubule mitochondrial injury and inflammation in chronic kidney disease. Nat Commun. 2023;14(1):3236. doi: 10.1038/ s41467-023-39050-y.

43 Dixon EE, Wu H, Muto Y, Wilson PC, Humphreys BD. Spatially resolved transcriptomic analysis of acute kidney injury in a female murine model. J Am Soc Nephrol. 2022;33(2):279–89. doi: 10.1681/ASN. 2021081150.

44 Onoda N, Kawabata A, Hasegawa K, Sakakura M, Urakawa I, Seki M, et al. Spatial and single-cell transcriptome analysis reveals changes in gene expression in response to drug perturbation in rat kidney. DNA Res. 2022;29(2):dsac007. doi: 10.1093/dnares/ dsac007.

45 Wang Z, Deng Q, Gu Y, Li M, Chen Y, Wang J, et al. Integrated single-nucleus sequencing and spatial architecture analysis identified distinct injured-proximal tubular types in calculi rats. Cell Biosci. 2023;13(1):92. doi: 10. 1186/s13578-023-01041-3.

46 Delorey TM, Ziegler CGK, Heimberg G, Normand R, Yang Y, Segerstolpe Å, et al. COVID-19 tissue atlases reveal SARS-CoV-2 pathology and cellular targets. Nature. 2021; 595(7865):107–13. doi: 10.1038/s41586-021-03570-8.

47 Smith KD, Prince DK, Henriksen KJ, Nicosia RF, Alpers CE, Akilesh S. Digital spatial profiling of collapsing glomerulopathy. Kidney Int. 2022;101(5):1017–26. doi: 10.1016/j. kint.2022.01.033.

48 Malone B, Urakova N, Snijder EJ, Campbell EA. Structures and functions of coronavirus replication-transcription complexes and their relevance for SARS-CoV-2 drug design. Nat Rev Mol Cell Biol. 2022;23(1):21–39. doi: 10. 1038/s41580-021-00432-z.

49 Salem F, Perin L, Sedrakyan S, Angeletti A, Ghiggeri GM, Coccia MC, et al. The spatially resolved transcriptional profile of acute T cell-mediated rejection in a kidney allograft.

Kidney Int. 2022;101(1):131–6. doi: 10.1016/ j.kint.2021.09.004.

50 Oszwald A, Mejia-Pedroza RA, Schachner H, Aigner C, Rees A, Kain R. Digital spatial profiling of glomerular gene expression in pauci-immune focal necrotizing glomerulonephritis. Kidney360. 2023;4(1):83–91. doi: 10.34067/KID. 000461202.

51 Ye L, Liu Y, Zhu X, Duan T, Wang C, Fu X, et al. Digital spatial profiling of individual glomeruli from patients with antineutrophil cytoplasmic autoantibody-associated glomerulonephritis. Front Immunol. 2022;13:831253. doi: 10.3389/ fimmu.2022.831253.

52 Hodgin JB, Borczuk AC, Nasr SH, Markowitz GS, Nair V, Martini S, et al. A molecular profile of focal segmental glomerulosclerosis from formalin-fixed, paraffin-embedded tissue. Am J Pathol. 2010;177(4):1674–86. doi: 10.2353/ajpath.2010.090746.

53 Smith KD, Akilesh S. Collapsing glomerulopathy: unraveling varied pathogeneses. Curr Opin Nephrol Hypertens. 2023;32(3):213–22. doi: 10.1097/MNH.0000000000000873.

54 Zimmerman SM, Fropf R, Kulasekara BR, Griswold M, Appelbe O, Bahrami A, et al. Spatially resolved whole transcriptome profiling in human and mouse tissue using Digital Spatial Profiling. Genome Res. 2022;32(10): 1892–905. doi: 10.1101/gr.276206.121.

55 Haug S, Muthusamy S, Li Y, Stewart G, Li X, Treppner M, et al. Multi-omic analysis of human kidney tissue identified medulla-specific gene expression patterns. Kidney Int. 2024;105(2):293–311. doi: 10.1016/j.kint. 2023.10.024.

56 Groelz D, Viertler C, Pabst D, Dettmann N, Zatloukal K. Impact of storage conditions on the quality of nucleic acids in paraffin embedded tissues. PLoS One. 2018;13(9): e0203608. doi: 10.1371/journal.pone. 0203608.

57 Risso D, Ngai J, Speed TP, Dudoit S. Normalization of RNA-seq data using factor analysis of control genes or samples. Nat Biotechnol. 2014;32(9):896–902. doi: 10. 1038/nbt.2931.

58 Hermsen M, de Bel T, den Boer M, Steenbergen EJ, Kers J, Florquin S, et al. Deep learning-based histopathologic assessment of kidney tissue. J Am Soc Nephrol. 2019;30(10):1968–79. doi: 10. 1681/ASN.2019020144.

59 Ginley B, Jen KY, Han SS, Rodrigues L, Jain S, Fogo AB, et al. Automated computational detection of interstitial fibrosis, tubular atrophy, and glomerulosclerosis. J Am Soc Nephrol. 2021;32(4):837–50. doi: 10.1681/ ASN.2020050652.

60 Ginley B, Lutnick B, Jen KY, Fogo AB, Jain S, Rosenberg A, et al. Computational segmentation and classification of diabetic glomerulosclerosis. J Am Soc Nephrol. 2019;30(10):1953–67. doi: 10.1681/ASN. 2018121259.

61 van Hijfte L, Geurts M, Vallentgoed WR, Eilers PHC, Sillevis Smitt PAE, Debets R, et al. Alternative normalization and analysis pipeline to address systematic bias in NanoString GeoMx Digital Spatial Profiling data. iScience. 2023;26(1):105760. doi: 10.1016/j.isci.2022.105760.

62 Bergholtz H, Carter JM, Cesano A, Cheang MCU, Church SE, Divakar P, et al. Best practices for spatial profiling for breast cancer research with the GeoMx® digital spatial profiler. Cancers. 2021;13(17):4456. doi: 10.3390/cancers13174456.

63 Lee TD, Aisner DL, David MP, Eno CC, Gagan J, Gocke CD, et al. Current clinical practices and challenges in molecular testing: a GOAL Consortium Hematopathology Working Group report. Blood Adv. 2023; 7(16):4599–607. doi: 10.1182/bloodadvances.2023010149.

64 Perou CM, Sørlie T, Eisen MB, van de Rijn M, Jeffrey SS, Rees CA, et al. Molecular portraits of human breast tumours. Nature. 2000; 406(6797):747–52. doi: 10.1038/35021093.

65 Paik S, Shak S, Tang G, Kim C, Baker J, Cronin M, et al. A multigene assay to predict recurrence of tamoxifen-treated, node-negative breast cancer. N Engl J Med. 2004;351(27): 2817–26. doi: 10.1056/NEJMoa041588.

66 Halloran PF, Madill-Thomsen KS, Reeve J. The molecular phenotype of kidney transplants: insights from the MMDx Project. Transplantation. 2024;108(1):45–71. doi: 10.1097/TP.0000000000004624.

67 Sikosana MLN, Reeve J, Madill-Thomsen KS, Halloran PF; INTERCOMEX Investigators. Using regression equations to enhance interpretation of histology lesions of kidney transplant rejection. Transplantation. 2024;108(2): 445–54. doi: 10.1097/TP.0000000000004783.

68 Reeve J, Bohmig GA, Eskandary F, Einecke G, Lefaucheur C, Loupy A, et al. Assessing rejection-related disease in kidney transplant biopsies based on archetypal analysis of molecular phenotypes. JCI Insight. 2017; 2(12):e94197. doi: 10.1172/jci.insight.94197.

69 Venner JM, Hidalgo LG, Famulski KS, Chang J, Halloran PF. The molecular landscape of antibody-mediated kidney transplant rejection: evidence for NK involvement through CD16a Fc receptors. Am J Transplant. 2015; 15(5):1336–48. doi: 10.1111/ajt.13115.

70 Sellares J, Reeve J, Loupy A, Mengel M, Sis B, Skene A, et al. Molecular diagnosis of antibody-mediated rejection in human kidney transplants. Am J Transplant. 2013;13(4): 971–83. doi: 10.1111/ajt.12150.

71 Mariani LH, Eddy S, AlAkwaa FM, McCown PJ, Harder JL, Nair V, et al. Precision nephrology identified tumor necrosis factor activation variability in minimal change disease and focal segmental glomerulosclerosis. Kidney Int. 2023;103(3):565–79. doi: 10.1016/j.kint.2022.10.023.

72 Bernard L, Wang AR, Menez S, Henderson JM, Dighe A, Roberts GV, et al. Kidney biopsy utility: patient and clinician perspectives from the kidney precision medicine Project. Kidney Med. 2023;5(10):100707. doi: 10.1016/j.xkme.2023.100707.

73 Trachtman H, Desmond H, Williams AL, Mariani LH, Eddy S, Ju W, et al. Rationale and design of the Nephrotic Syndrome Study Network (NEPTUNE) Match in glomerular diseases: designing the right trial for the right patient, today. Kidney Int. 2024; 105(2):218–30. doi: 10.1016/j.kint.2023.11.018.

74 Dominy KM, Roufosse C, de Kort H, Willicombe M, Brookes P, Behmoaras JV, et al. Use of quantitative real time polymerase chain reaction to assess gene transcripts associated with antibody-mediated rejection of kidney transplants. Transplantation. 2015;99(9): 1981–8. doi: 10.1097/TP.0000000000000621.

75 Miller MB, Watts ML, Samuel L. FDA's proposed rule for the regulation of laboratory-developed tests. J Clin Microbiol. 2024;62(2):e0148823. doi: 10.1128/jcm.01488-23.

76 Cang Z, Zhao Y, Almet AA, Stabell A, Ramos R, Plikus MV, et al. Screening cell-cell communication in spatial transcriptomics via collective optimal transport. Nat Methods. 2023;20(2):218–28. doi: 10.1038/s41592-022-01728-4.

77 Kim H, Kumar A, Lovkvist C, Palma AM, Martin P, Kim J, et al. CellNeighborEX: deciphering neighbor-dependent gene expression from spatial transcriptomics data. Mol Syst Biol. 2023;19(11):e11670. doi: 10.15252/msb.202311670.